A Journal of the Gesellschaft Deutscher Chemiker

Angewandte International Edition Chemie

GDCh

www.angewandte.org

Accepted Article

Title: Efficient Intramolecular Charge-Transfer Fluorophores Based on Substituted Triphenylphosphine Donors

Authors: Zhang Liu, Chao Deng, Liwu Su, Dan Wang, Yongshi Jiang, Taiju Tsuboi, and Qisheng Zhang

To be cited as: *Angew. Chem. Int. Ed.* 10.1002/anie.202103075

Link to VoR: https://doi.org/10.1002/anie.202103075

WILEY-VCH

10.1002/anie.202103075

WILEY-VCH

Efficient Intramolecular Charge-Transfer Fluorophores Based on Substituted Triphenylphosphine Donors

Zhang Liu,[a] Chao Deng,[a] Liwu Su,[a] Dan Wang,[a] Yongshi Jiang,[a] Taiju Tsuboi,[a] Qisheng Zhang*[ab]

[a] Z. Liu, Dr. C. Deng, L. Su, Dr. D. Wang, Y. Jiang, Prof. T. Tsuboi, Prof. Q. Zhang
MOE Key Laboratory of Macromolecular Synthesis and Functionalization
Department of Polymer Science and Engineering, Zhejiang University
Hangzhou 310027, China
E-mail: qishengzhang@zju.edu.cn
[b] Prof. Q. Zhang
State Key Laboratory of Clean Energy Utilization
Zhejiang University
Hangzhou 310027, China

Abstract: Triphenylphosphine (TPP)-based luminescent compounds are rarely investigated because of the low photoluminescence quantum yield (PLQY). Here, we demonstrate that introducing steric hindrance groups to the TPP moiety and separating the orbitals involved in the transition can drastically suppress the non-radiative decay induced by structural distortion of TPP in the excited state. High PLQY up to 0.89 as well as thermally activated delayed fluorescence are observed from the intramolecular charge-transfer (ICT) molecules with substituted TPP donors (sTPPs) in doped films. The red organic light-emitting diodes employing these emitters achieve comparable external quantum efficiencies to the control device containing a classical phosphorescent dye, revealing the great potential of the ICT emitters based on electrochemically stable sTPPs.

Organic molecules with intramolecular charge-transfer (ICT) excited states have been extensively investigated due to their potential applications in organic light emitting diodes (OLEDs),[1] solar energy conversion,[2] non-linear optics,[3] fluorescent probes and sensors.[4] In recent years, specially designed ICT molecules with small energy differences between their first singlet and triplet excited states (ΔE_{ST}) have received growing attention, because the OLEDs employing them can effectively convert dark triplet excitons into emissive singlet ones and achieve nearly 100% internal quantum efficiency without using noble metals like iridium and platinum.[5] These ICT emitters typically exhibit thermally activated delayed fluorescence (TADF) at room temperature (RT) and are described as TADF materials. To date, triphenylamines (TPA) and their derivatives have been widely used as donors in ICT molecules.[1-5] However, there are few reported examples of an ICT molecule with a non-nitrogenous donor. In 2019, Su *et al.* suggested a new thianthrene donor based on sulfur and constructed a green TADF emitter, which simultaneously exhibits ICT and intermolecular charge transfer through space.[6]

Within the same main group, phosphorus ($3s^23p^3$) and nitrogen ($2s^22p^3$) share a similar valence electron configuration. However, triphenylphosphine (TPP) is not considered an appropriate electron-donating fragment for the construction of metal-free ICT emitters because of its deep highest occupied molecular orbital (HOMO).[7] In TPA, the centered nitrogen takes a planar sp^2 hybridization due to steric hindrance effects. The nitrogen $2p_z$ orbital without hybrid stabilization contributes to the HOMO together with the 2p orbitals in the phenyl rings, leading to a shallow HOMO in TPA.[8] In contrast, the long C-P bonds in TPP allow TPP a pyramid configuration and nonequivalent sp^3 hybridization in phosphorus atom.[9] The lone electron pair consisting of a high ratio of 3s/3p leads to the relatively deep HOMO level. Moreover, trivalent phosphines may suffer from severe structural deformation and configuration flips in excited state,[10] which would accelerate the non-radiative decay and decrease the photoluminescence quantum yield (PLQY). Due to this quenching effect, efficient emitters based on trivalent phosphorus compounds have not yet been reported.

In 1975, Blount *et al.* analyzed a single-crystal structure of trimesitylphosphine (TMP) and found that the methyl groups in the *o*-position to the P atom increase the steric hindrance and lead to a more planar geometry around P.[11] In 1980, A.V. Il'yasov *et al.* observed a highly reversible electrochemical reaction in TMP with a low oxidation potential.[12] In 2002, Sasaki *et al*. replaced the methyl groups in TMP to bulk isopropyl groups and obtained a near planar TPP derivative—tris(2,4,6-triisopropylphenyl)phosphine—that has a shallower HOMO level and improved electrochemical stability relative to TMP.[13] Sasaki *et al*. demonstrated that substituted TPP can undergo Sonogashira and Suzuki-Miyaura coupling with common pallidum catalysts and successfully obtained several emissive compounds, although the PLQYs of these compounds are still low (0.02%−1.7%).[14] In this work, a series of ICT molecules with substituted TPP donors (sTPPs) and a triazine acceptor were synthesized. Decreasing the electron-hole wavefunctions overlap at the excited state was found to be an effective strategy to suppress the non-radiative decay caused by the structural deformation of the donor moiety. These phosphorus-based emitters exhibit efficient TADF in doped films and afford orange-red OLEDs with external quantum efficiencies (EQEs) far beyond traditional fluorescence OLEDs, indicating that electrochemically stable sTPPs have emerged as competitors to conventional TPA for efficient photoluminescent (PL) and electroluminescent (EL) materials.

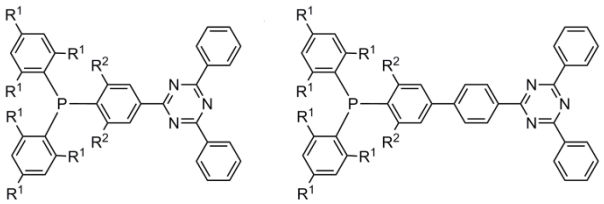

a1 $R^1 = R^2 = H$
a2 $R^1 = CH_3$; $R^2 = H$
a3 $R^1 = R^2 = CH_3$
a4 $R^1 = CH(CH_3)_2$; $R^2 = CH_3$

b1 $R^1 = R^2 = H$
b2 $R^1 = CH_3$; $R^2 = H$
b3 $R^1 = R^2 = CH_3$
b4 $R^1 = CH(CH_3)_2$; $R^2 = CH_3$

Figure 1. Molecular structures of compounds **a1−4** and **b1−4**.

Eight dipolar molecules without (**a1**–**4**) and with (**b1**–**4**) a phenyl-bridge were designed and synthesized via TPP substituted with different steric hindrance groups as the donor and high triplet energy 2,4-diphenyl-1,3,5-triazine as acceptor (Figure 1). The geometry optimization of the S_0 states was performed using density functional theory (DFT) at B3LYP/6-31G(d) level in Gaussian 09 program package. The calculation indicates that the TPP donor in **a1** and **b1** takes a pyramid configuration as in individual TPP (Figures 2a and S1). The increase in steric hindrance around the P forces the TPP segment into a planar propeller structure (Table S1) and changes the hybridization of P-atom orbitals from sp^3 to sp^2 (Table S2). The decrease in the contribution of the atomic 3s orbital to the hybridized lone-pair orbital enhances the HOMO energy level of the TPP derivatives.[15] Meanwhile, the HOMO becomes more localized towards the phosphorus center with increased steric hindrance around the P-atom (Figure 2a). The S_1 transitions were simulated at the ground state geometries by time-dependent DFT at the mpw1b95/6-31G(d,p) level (Table S3). The ΔE_{ST} values reduced from 0.81 eV for **b1** to 0.43 eV for **b4** with a decrease in the orbital overlap between HOMO and LUMO. However, even for **b4** that exhibits the smallest orbital overlap, the calculated oscillator strength (*f*) of the S_1 transition is still as large as 0.47 (Figure 2a) implying a large fluorescence rate.

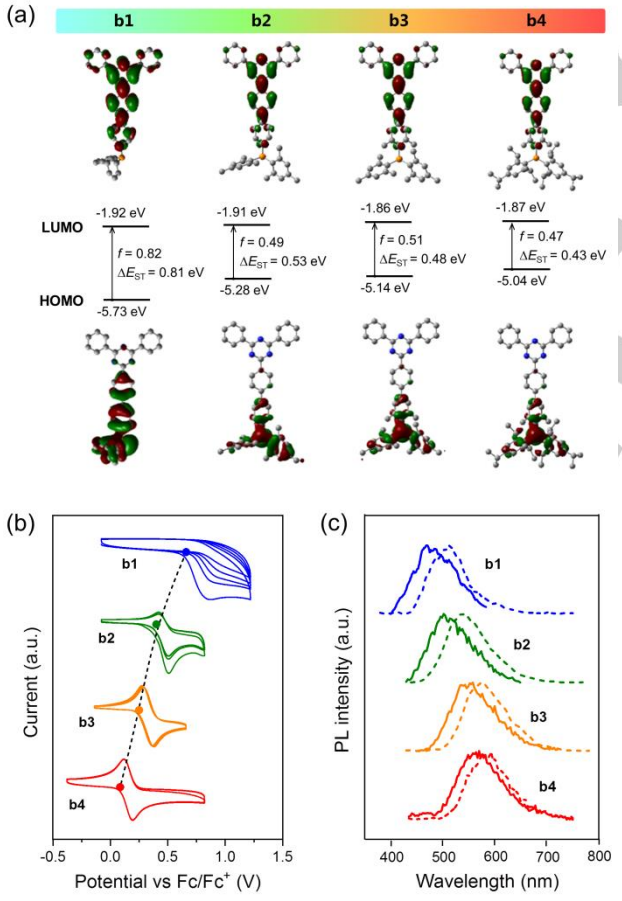

Figure 2. (a) Computed HOMO and LUMO distributions, orbital energies, oscillator strengths of S_1 transition, and exchange energies between S_1 and T_1 transitions. The ground state geometries are optimized at the DFT/B3LYP/6-31G(d) level. (b) Multiple scan cyclic voltammograms for the oxidation of **b1**−**4** in dichloromethane at RT. (c) Fluorescence (1 ns) and phosphorescence spectra (0.1−1 ms) in toluene at 77 K.

The synthesis routes towards these TPP-based emitters are shown in the Supporting Information. Species **a1** and **b1** were synthesized via a reaction of sodium diphenylphosphanide with fluoride intermediates. The substituents around the phosphorus reduce the coordination ability of the lone electron pair on the P-center, thus allowing an efficient Suzuki-Miyaura coupling to yield **a2**−**4** and **b2**−**4**. Enlarging the steric hindrance around the P leads to a chemical shift of ^{31}P-NMR to high-field (*e.g.*, -5.1 ppm, -22.7 ppm, -35.7 ppm, and -46.6 ppm for **b1**, **b2**, **b3**, and **b4**, respectively), indicating an increase in the electron density around phosphorus nuclei as predicted by DFT calculations.

The electrochemical properties of these TPP-based emitters were investigated by cyclic voltammetry. Species **a1** and **b1** contain an unsubstituted TPP donor and exhibit an irreversible oxidation behavior. The reversibility of the redox reactions improves with increasing steric protection of the P-center (Figures 2b and S2). In contrast, the nitrogen atom in the TPA derivatives cannot have similar protection because of the shorter C-N bonds resulting in relatively poor electrochemical stability versus substituted TPP derivatives (Figure S3). In accordance with the calculation results, the oxidation potentials of these TPP-based ICT molecules can be significantly reduced by increasing the steric hindrance around the phosphor core (Figure 2b). The oxidation potentials of 0.07 eV for **b4** (vs Fc/Fc^+) is even higher than that of its analogues (TPA-Ph-TRZ) with a conventional TPA donor (0.25 eV, see Figure S3).

The eight emitters exhibit broad and smooth PL emission spectra in toluene at RT with peaks (λ_{PL}) ranging from 518 nm to 647 nm (Figure S4). A significant bathochromic effect was observed with increasing solvent polarity indicating the ICT nature of the transition (Figure S4). In accordance with the theoretical prediction, the bands of emission and first absorption (Figure S5) are redshifted by increasing the steric hindrance of the substituents on the TPP donor. The ΔE_{ST} values of the eight emitters in toluene were estimated from the energy difference between the onset of the fluorescence and phosphorescence spectra at 77 K (Figure 2c and S6). Increasing steric hindrance around the P-center and enlarging the donor-acceptor (D-A) distance significantly diminishes ΔE_{ST} from 0.26 eV for **a1** to 0.11 eV for **b4** (Table 1). The experimental values of ΔE_{ST} are distinctly smaller than the theoretical ones that are calculated as the energy difference between the vertical transitions of $S_0 \rightarrow S_1$ and $S_0 \rightarrow T_1$ (Figure 2a), implying a large difference between the geometries in the ground and excited states.

Table 1. Photo- and electro-luminescent properties of TPP-based emitters

Comp.	λ_{PL} [nm] [a] sol/ film	PLQY [a] sol/ film	ΔE_{ST} [b] [eV]	λ_{EL} [nm]	EQE_{max} [%]	R_{EP} [c]
a1	568/ 481	0.04/ 0.19	0.26	508	2.0	0.11
a2	595/ 532	0.04/ 0.74	0.26	535	8.4	0.11
a3	637/ 588	0.03/ 0.58	0.21	606	10.1	0.17
a4	647/ 605	0.03/ 0.38	0.18	626	6.9	0.18
b1	518/ 446	0.05/ 0.40	0.25	493	4.5	0.11
b2	541/ 520	0.22/ 0.89	0.20	516	10.1	0.11
b3	597/ 563	0.24/ 0.71	0.15	586	13.6	0.19
b4	620/ 578	0.17/ 0.56	0.11	614	12.0	0.21

[a] Measured in toluene (0.1 mM) and doped mCP films (10 wt%) at RT; [b] Measured in toluene at 77 K; [c] $R_{EP} = EQE_{max}/PLQY$

Interestingly, inserting a phenyl-bridge between the donor and acceptor can drastically boost the PLQYs from 0.03–0.04 for **a2**–**4** to 0.17–0.24 for **b2**–**4** in degassed toluene (Table 1). The efficiency improvement can be attributed to the effective non-radiative decay suppression by reducing the influence of donor deformation on the electronic structure at the separated acceptor.[16] Figure 3a shows the picosecond fluorescence decay dynamics of **a3** and **b3** in toluene at RT. The excited-state relaxation-induced ultrafast fluorescence decay on the time scale of a few picoseconds is only observed in the solution of **3a**. The low PLQY of **b1** is interpreted as a strong electric coupling between donor and acceptor, which is reflected in the relatively large overlap of HOMO and LUMO (Figure 2a).

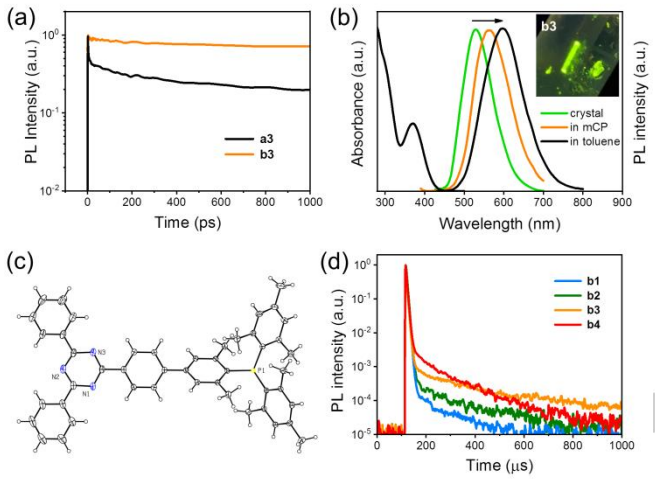

Figure 3. (a) Ultrafast fluorescence decay spectra of **a3** and **b3** in toluene at RT. (b) Absorption spectrum of **b3** in toluene and PL spectra of **b3** in crystal, toluene and 10 wt% doped mCP film at RT. (c) Crystal structure of **b3** (50% probability ellipsoids). (d) Transient decay spectra of **b1**−**4** in 10 wt % doped mCP films at RT.

The single crystal of **b3** exhibits nearly 100% PLQY with an obviously blue-shifted and narrowed emission band relative to that in solution (Figure 3b) confirming that the relatively low PLQY in solution is related to the excited-state geometry changes. The three C-P-C bond angles in the **b3** crystal are determined to be 106.8°, 112.1°, and 111.9° by X-ray structural analysis (Figure 3c), obviously deviating from the sp^3 pyramid configuration. The 46.7° dihedral angle between the triphenyltriazine plane and a phenyl group on the TPP donor is responsible for the effective separation of the hole and electron in excited **3b**. No close π-π stacking is observed in the packing diagram of **3b** (Figure S7) due to the bulk TMP donor in it.

The emission maximum (563 nm) and PLQY (0.71) of **3b** doped in m-bis(N-carbazolyl)benzene (mCP) film (10 wt%) fall in between the corresponding values in crystal and toluene indicating that structural distortion-induced non-radiative decay could be largely suppressed in solid films. An approximate inverse relation between PLQY and peak emission wavelength (Table 1) is found in the six emitters with sTPPs (**a2**−**a4** and **b2**−**b4**) in doped films, suggesting that the non-radiative decay in films is governed by the energy gap law. The highest PLQY of 0.89 is achieved by **b2** in the film with an emission maximum of 520 nm. Even in solid films, the PLQYs of the unsubstituted TPP molecules (**a1** and **b1**) are much lower than those of the substituted TPP molecules (Table 1). Slow components with lifetimes on the order of 100 μs were observed in the transient decay spectra of the doped films at RT (Figures 3d and S8). The delayed fluorescence is caused by the reverse intersystem crossing from T_1 to the emissive S_1 as confirmed by the temperature dependent transient spectra (Figure S9). The relatively long lifetimes (Table S5) can be ascribed to the relatively large ΔE_{ST} over 0.11 eV (Table 1) for these emitters.[5e] With increased steric hindrance in the donor, the TADF component increases while the lifetime decreases due to the decrease in ΔE_{ST} of these compounds.

The decomposition temperatures (corresponding to the 5% weight loss) of the 8 TPP-based emitters are all above 350 ºC (Figure S10) satisfying the requirement of vacuum deposition technique used in OLED fabrication. Purities of the compounds after sublimation were determined to be over 99% by a high-performance liquid chromatographic method (Figure S11). As shown in Figure S12, introducing steric hindrance groups to the TPP moiety can enhance the glass transition temperatures from 59 °C for **a1** and 81 °C for **b1** to 113 °C for **a3** and 120 °C for **b3**, affording high thermal stability for these TPP donor-based emitters in organic films.

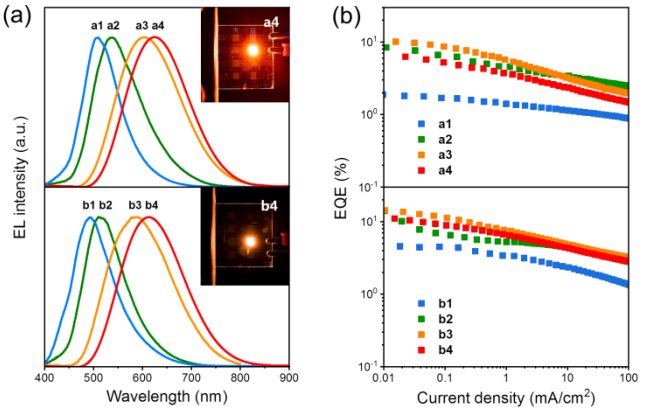

Figure 4. Performance of the OLEDs employing different emitters. (a) EL spectra at 10 mA/cm^2. Inset: Images of the **a4**- and **b4**-based OLEDs. (b) EQE-current density characteristics.

The EL properties of these emitters were evaluated with a device structure of ITO/HAT-CN (10 nm)/TAPC (40 nm)/TCTA (10 nm)/Tris-Pcz: $Bepp_2$: emitter (30 wt%: 60 wt%: 10 wt%, 30 nm)/$Bepp_2$ (60 nm)/Li_2CO_3 (1 nm)/Al (Figure S13) where high triplet energy bis[2-(2-hydroxyphenyl)-pyridine]beryllium ($Bepp_2$) and 9,9',9''-triphenyl-9H,9'H,9''H-3,3':6',3''-tercarbazole (Tris-Pcz) are the co-host matrix for the emitter. The 1,1-bis[(di-4-tolylamino)phenyl] cyclohexane (TAPC) and tris(4-carbazoyl-9-ylphenyl)amine (TCTA) are used as the hole-transport layers, and 1,4,5,8,9,11-hexaazatriphenylenehexacarbonitrile (HAT-CN), $Bepp_2$, and Li_2CO_3 are used as the hole-injection, electron-transport, and electron-injection layers, respectively. These devices turn on at approximate 2.8 V with tunable emission color from bluish green to red (Figures 4a and S14). The orange and orange-red devices containing **b3** and **b4** show a maximum EQE (EQE_{max}) of 13.6% and 12.0%, respectively, that are comparable to the device containing a classical red

phosphorescent emitter tris[1-phenylisoquinolinato-C2,N]iridium (III) ($Ir(piq)_3$, see Figure S15).[17] The ratio of EQE_{max} to PLQY (R_{EP}) for these TPP donor-based emitters significantly increases with increasing steric hindrance in their donor moiety (Table 1) to approach a theoretical upper limit of 20-30% given by the following formula,

$$EQE/PLQY = \gamma \eta_r \eta_{out}$$

where the upper limits of the electron/hole recombination ratio (γ) and the exciton formation ratio for radiative transitions (η_r) are 100%, and the light out-coupling efficiency (η_{out}) is generally in the range of 20-30%.[18] For comparison, the device employing TPA-Ph-TRZ, the analogues of **b1** with a TPA donor, was also fabricated. Although the PLQY of TPA-Ph-TRZ in doped mCP film is as high as 0.87, the EQE_{max} of its devices is less than 5% (Figure S16).

Although the above device structure has not been fully optimized for long lifetime, the half-lifetimes of the devices containing sTPPs-based emitters can reach a few hours at an initial luminescence of 500 cd/m^2 (Figure S17), which are comparable to those of the early reported TADF OLEDs containing phenylamine donor-based emitters.[19] Note that the large structural distortion of TPP-donors in their oxidation state leads to large reorganization energies during hole transport (Figure S14), which would trap holes on the emitters and result in polaron-exciton-induced degradation in OLEDs.[20] Developing EL materials containing rigid and plane phosphorus-based functional groups is under way.

In short, sTPPs exhibiting good electrochemical reversibility are an alternative to the traditional TPA donor in the design of novel ICT transition emitters. The introduction of steric groups to TPP donor can suppress the structural deformation in the excited state and increases the PLQY of the emitter. In addition, enlarging the D-A distance can significantly improve the PLQY of sTPPs-based emitters in solution by blocking the non-radiative decay channel associated with donor distortion. Owing to the small HOMO/LUMO overlap and high local triplet excited state energy, the ICT molecules with sTPPs emit TADF in doped films and they can harvest both singlet and triplet excitons in OLEDs. An orange red OLED containing a TADF emitter with an isopropyl-substituted TPP donor realizes an EQE_{max} of 12.0%, which is comparable to that of the device containing a classical red phosphor.

Acknowledgements

This work is supported by the National Natural Science Foundation of China (Grant No. 51873183) and the National Key R&D Program of China (Grant No. 2016YFB0401004).

Conflict of interest

The authors declare no conflict of interest.

Keywords: triphenylphosphine donor • intramolecular charge transfer • organic light emitting diodes • thermally activated delayed fluorescence • non-radiative decay

[1] a) C. Chen, *Chem. Mater.* **2004**, *16*, 4389−4400; b) A. Chaskar, H. Chen, K. Wong, *Adv. Mater.* **2011**, *23*, 3876−3895; c) X. Yang, X. Xu, G. Zhou, *J. Mater. Chem. C* **2015**, *3*, 913−944.

[2] a) Y. Wu, W. Zhu, *Chem. Soc. Rev.* **2013**, *42*, 2039−2058; b) H. Meier, Z. Huang, D. Cao, *J. Mater. Chem. C* **2017**, *5*, 9828−9837; c) D. Dang, D. Yu, E. Wang, *Adv. Mater.* **2019**, *31*, 1807019.

[3] a) S. Kannan, A. Sekar, K. Sivaperuman, *J. Mater. Chem. C* **2020**, *8*, 16668−16690; b) S. Sasaki, G. P. Drummen, G. Konishi, *J. Mater. Chem. C* **2016**, *4*, 2731−2743.

[4] a) X. Li, X. Gao, W. Shi, H. Ma, *Chem. Rev.* **2014**, *114*, 590−659; b) D. Wu, A. C. Sedgwick, T. Gunnlaugsson, E. U. Akkaya, J. Yoon, T. D. James, *Chem. Soc. Rev.* **2017**, *46*, 7105−7123.

[5] a) X. Cai, S. Su, *Adv. Funct. Mater.* **2018**, *28*, 1802558; b) J. H. Kim, J. H. Yun, J. Y. Lee, *Adv. Optical Mater.* **2018**, *6*, 1800255; c) Y. Liu, C. Li, Z. Ren, S. Yan, M. R. Bryce, *Nat. Rev. Mater.* **2018,** *3,* 18020; d) J. Li, T. Nakagawa, J. MacDonald, Q. Zhang, H. Nomura, H. Miyazaki, C. Adachi, *Adv. Mater.* **2013**, *25*, 3319; e) Q. Zhang, H. Kuwabara, Jr. W. J. Potscavage, S. Huang, Y. Hatae, T. Shibata, C. Adachi, *J. Am. Chem. Soc.* **2014,** *136,* 18070−18081; f) D. Zhang, M. Cai, Y. Zhang, D. Zhang, L. Duan, *Mater. Horiz.* **2016**, *3*, 145−151; g) C. Li, R. Duan, B. Liang, G. Han, S. Wang, K. Ye, Y. Liu, Y. Yi, Y. Wang, *Angew. Chem. Int. Ed.* **2017**, *56*, 11525−11529; h) B. Zhao, H. Wang, C. Han, P. Ma, Z. Li, P. Chang, H. Xu, *Angew. Chem. Int. Ed.* **2020**, *59*, 19042−19047.

[6] X. Cai, Z. Qiao, M. Li, X. Wu, Y. He, X. Jiang, Y. Cao, S. J. Su, *Angew. Chem. Int. Ed.* **2019**, *58*, 13522−13531.

[7] a) J. Wang, X. Xu, Y. Tian, C. Yao, R. Liu, L. Li, *J. Mater. Chem. C* **2015**, *3*, 2856−2864; b) Y. Li, Y. Kang, S. Ko, Y. Rao, F. Sauriol, S. Wang, *Organometallics* **2013**, *32*, 3063−3068.

[8] T. Zhang, I. E. Brumboiu, C. Grazioli, A. Guarnaccio, M. Coreno, M. de Simone, A. Santagata, H. Rensmo, B. Brena, V. Lanzilotto, C. Puglia, *J. Phys. Chem. C* **2018**, *122*, 17706−17717.

[9] a) J. J. Daly, *Z. Kristallogr. Cryst. Mater.* **1963**, *118*, 332−333; b) J. J. Daly, *J. Chem. Soc.* **1964**, 3799−3810.

[10] a) R. T. Boeré, A. M. Bond, S. Cronin, N. W. Duffy, P. Hazendonk, J. D. Masuda, K. Pollard, T. L. Roemmele, P. Tran, Y. Zhang, *New J. Chem.* **2008**, *32*, 214−231; b) K. D. Reichl, D. H. Ess, A. T. Radosevich, *J. Am. Chem. Soc.* **2013**, *135*, 9354−9357; c) K. Fujimoto, A. Osuka, *Chem. Sci.* **2017**, *8*, 8231−8239; d) T. Machida, T. Iwasa, T. Taketsugu, K. Sada, K. Kokado, *Chem. Eur. J.* **2020**, *26*, 8028−8034.

[11] J. F. Blount, C. A. Maryanoff, K. Mislow, *Tetrahedron Lett.* **1975**, *16*, 913−916.

[12] A. V. Il'yasov, Y. M. Kargin, E. V. Nikitin, A. A. Vafina, G. V. Romanov, O. V. Parakin, A. A. Kazakova, A. N. Pudovik, *Phosphorus, Sulfur Silicon Relat. Elem.* **1980**, *8*, 259−262.

[13] S. Sasaki, K. Sutoh, F. Murakami, M. Yoshifuji, *J. Am. Chem. Soc.* **2002**, *124*, 14830−14831.

[14] a) S. Sasaki, *Tetrahedron Lett.* **2018**, *59*, 2251−2255; b) S. Sasaki, K. Kato, K. Sasaki, M. Yoshifuji, *Tetrahedron Lett.* **2020**, *61*, 151366; c) S. Sasaki, K. Ogawa, K. Nakamura, M. Yoshifuji, N. Morita, *J. Organomet. Chem.* **2014**, *751*, 525−533; d) S. Sasaki, K. Sasaki, M. Yoshifuji, *J. Organomet. Chem.* **2011**, *696*, 3307−3315; e) S. Sasaki, M. Yoshifuji, *Curr. Org. Chem.* **2007**, *11*, 17−31.

[15] J. M. Osawa, M. Hoshino, T. Wada, Y. Araki, O. Ito, *Chem. Phys. Lett.* **2006**, *427*, 338−342.

[16] J. Liu, K. Zhou, D. Wang, C. Deng, K. Duan, Q. Ai, Q. Zhang, *Front. Chem.* **2019**, *7*, 312.

[17] A. Tsuboyama, H. Iwawaki, M. Furugori, T. Mukaide, J. Kamatani, S. Igawa, T. Moriyama, S. Miura, T. Takiguchi, S. Okada, M. Hoshino, K. Ueno, *J. Am. Chem. Soc.* **2003**, *125*, 12971.

[18] K. Saxena, V. K. Jain, D. S. Mehta, *Opt. Mater.* **2009**, *32*, 221−233.

[19] a) Q. Zhang, D. Tsang, H. Kuwabara, Y. Hatae, B. Li, T. Takahashi, S. Y. Lee, T. Yasuda, C. Adachi, *Adv. Mater.* **2015**, *27*, 2096−2100; b) L.-S. Cui, Y.-L. Deng, D. P.-K. Tsang, Z.-Q. Jiang, Q. Zhang , L.-S. Liao, C. Adachi, *Adv. Mater.* **2016**, *28*, 7620−7625.

[20] Q. Niu, R. Rohloff, G. A. H. Wetzelaer, P. W. M. Blom, N. I. Craciu, *Nat. Mater.* **2018**, *17*, 557–562.

10.1002/anie.202103075

Entry for the Table of Contents

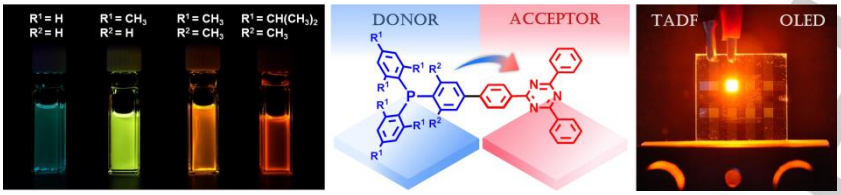

Trivalent phosphorus is considered as new electron donating species for intramolecular charge transfer fluorophores. The efficient triphenylphosphine-based emitters with excellent electrochemical stability and small singlet-triplet splitting afford potentials for luminescence-based applications and devices.